Inflence of Grain Arrangement and Crack Propagation Path on Crack Propagation Rate in Fatigue of Directionally Solidified Superalloy

M. Yamamoto[1], T. Kitamura[2], T. Ogata[3]

[1] Central Research Institute of Electric Power Industry, 2-11-1, Iwado-kita, Komae, Tokyo, JAPAN, 201-8511, masatoy@criepi.denken.or.jp
[2] Graduate School of Kyoto University, Yoshida-honmachi, Sakyo-ku, Kyoto, Kyoto, JAPAN, 606-8501, kitamura@kues.kyoto-u.ac.jp
[3] Central Research Institute of Electric Power Industry, togata@criepi.denken.or.jp

ABSTRACT. *The fluctuation of J-integral, J, during high temperature fatigue crack propagation, due to the microscopic inclination of crack shape and elastic anisotropy of each grain, is investigated by means of a series of finite-element-analyses on a cracked body. The simulated material is a Nickel-based directionally solidified (DS) superalloy, where the DS, load, and crack propagation axes are set to be perpendicular to each other. The magnitude of J is estimated using 2-dimensional models simulated after an experimental result; (i) with the actual crack shape and grain arrangement, (ii) with the actual crack shape in the homogeneous body, and (iii) with the straight crack in homogeneous body (averaged deformation behavior of the material). The microscopic inclination of crack propagation direction causes the sporadic drop of J at the point where the crack direction is largely inclined from the direction normal to the load axis. The anisotropy of grain causes the stepwise change in the a (crack length) - J relationship. These directly relate to the change in the crack propagation rate in the transgranular cracking. Then, J, which takes into accounts the factors, correlates well with the crack propagation rate in the transgranular cracking. The grain-boundary cracking possesses fluctuated J and shows weaker resistance against the propagation than the transgranular one.*

INTRODUCTION

On a macroscopic scale, though the fatigue crack propagation in a polycrystalline superalloy is governed by the effective stress intensity factor range, ΔK_{eff} [1-3], it have eminent fluctuation on a microscopic scale due to the network of grain boundaries [4-8]. In other words, the grain is one of the strongest influential factors on the propagation. ΔK_{eff} is also applicable to the crack propagation in a single-crystal superalloy [9-16]. However, little research work has been carried out on the fatigue crack growth behavior of directionally solidified (DS) superalloys from the viewpoint of fracture mechanics [17-19]. The grain size of DS superalloy is more than 100 mm on the major and about

0.2 to 5 mm on the minor axis. As these are in the same order of length as a main crack in a real component, the inhomogeneity and anisotropy due to the aligned multi-grains may give characteristic influence on the propagation in fatigue.

In this research, the effects of microstructure (the microscopic inclination of crack shape and the elastic anisotropy of each grain) on the fracture mechanics parameter are investigated by means of an elastic finite element analysis (FEA).

CRACK PROPAGATION PROPERTY EXPERIMENTALLY OBSERVED IN A HIGH-TEMPERATURE FATIGUE OF DS SUPERALLOY [20]

In a previous paper, authors reported the crack propagation property in a high temperature fatigue of a γ/γ'-precipitation-strengthened DS superalloy, whose chemical composition is C-0.10, Al-3.03, B-0.02, Co-9.56, Cr-13.93, Mo-1.56, Ta-2.77, Ti-4.90, W-3.86, Zr-0.01, Ni-Bal, in wt%. Here, a crack-centered-plate specimen (Fig. 1(a)), where the DS axis was set to be perpendicular to the flat section, was subjected to a load-controlled uni-axial cyclic loading under the temperature of 1143K. The loading waveform was triangular with the Max. / Min. stresses of 400, and -200MPa, respectively, with the frequency of 0.13 Hz. The crack propagation behavior, which had no effect of creep, was carefully observed during the test and the crack propagation rate, *da/dN*, against the crack length was obtained as shown in Fig. 2. Here, *a* is the half crack length along the *x* axis (Fig. 1(b)). The crack propagation rate fluctuated during the crack propagation. The notable fluctuation of *da/dN* was observed in the intergranular cracking, while the transgranular cracking showed the averaged *da/dN*. At the peak of fluctuation, *da/dN* was accelerated to 10^{-2} [mm/cycle] at *a*=1.3mm which was 10 times faster than the average.

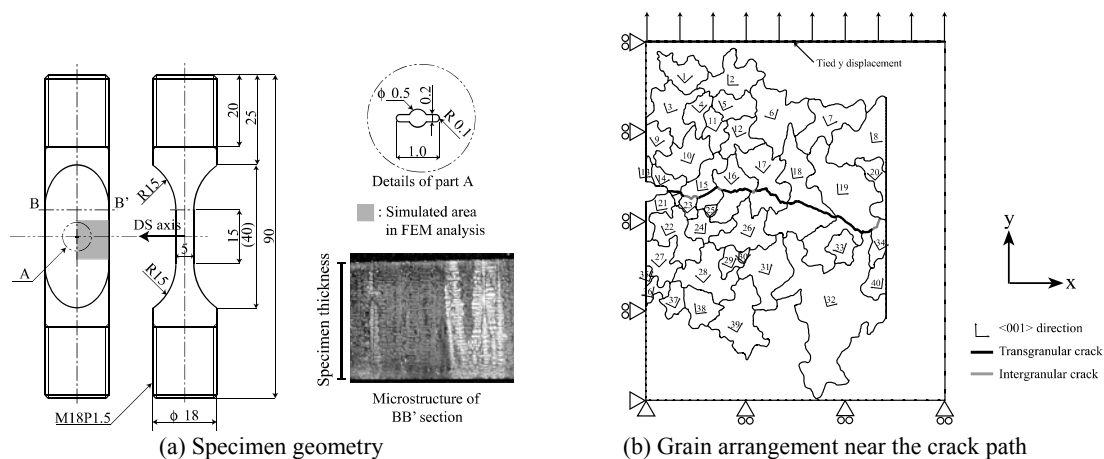(a) Specimen geometry   (b) Grain arrangement near the crack path

Fig. 1 Geometry of center-cracked plate specimen, crack profile with grain sketch, and the boundary condition of FEA
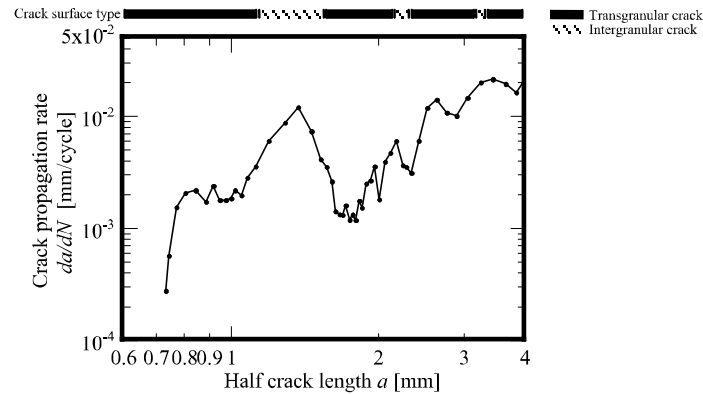
Fig.2 Crack propagation property obtained by a fatigue crack propagation test

The flat surface of the specimen was mechanically and electro-chemically polished after the crack propagation test in order to remove the oxidation. Then, the distribution of crystallographic orientation was evaluated by means of an Electron-Back-Scattering-diffraction-Pattern (EBSP). Figure 1(b) shows the grain arrangement and its crystallographic orientations on the specimen surface. The fatigue crack path was also traced out.
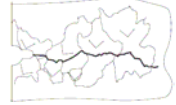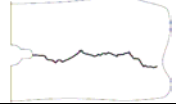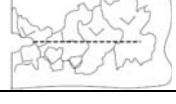
ANALYTICAL PROCEDURE

Finite element analyses (FEA) are carried out using a general-purpose FEA code, MSC/MARC 2003. Boundary conditions are shown in Fig. 1(b). The homogeneous remote tensile stress of 400MPa is applied controlling the y-displacements at the nodes of upper end. Since the tested material is in the small-scale-yielding condition during the fatigue loading, the analyses are conducted under the linear elastic condition. Here, J-integral [21], J, is employed as a fracture mechanics parameter which represents the driving force of crack propagation.

In order to clarify the total effects of the elastic anisotropy of real grains and the microscopic inclination of crack shape on the magnitude of J, 3 types of analyses listed in Table 1 are conducted;

(i) Analysis considering the grain arrangement and the microscopic inclination of crack shape

(ii) Analysis for the microscopically inclined crack in the homogeneous body

(iii) Analysis for the straight crack in the homogeneous body

Although there is inhomogeneity in smaller scale such as dendrite or γ/γ' structure, the effect is out of scope in this paper. The effects of smaller scale inhomogeneity are involved in the material constants; the crack propagation resistance of material.

Table 1 Definition of calculated J integral

Model No.	Symbol	Model	Crack shape	Material property	Description
(i)	J_{aniso}		Actual	Multi-grains, anisotropic	Energy release rate supporting both effects of the "microscopic anisotropy" related to grain arrangement and the "microscopic inclination of crack shape"
(ii)	J_{iso}		Actual	Isotropic	Energy release rate supporting the effect of "microscopic inclination of crack shape"
(iii)	$J_{straight}$		Straight	Isotropic	Energy release rate of straight crack in homogeneous and isotropic material
(iv)	J_{grain}		Straight	Multi-grains, anisotropic	Energy release rate supporting the effect of "microscopic anisotropy" related to grain arrangement

Analysis (i) simulates the grain shape and its anisotropic stiffness within the area of 3 or 4 grains near the crack. Here, the elastic stiffness in each grain is given as C_{11}=201.5, C_{12}=137.1, and C_{44}=98.5 (unit in GPa), which are evaluated by interpolating those in the pure γ and pure γ' [22] for the γ'-volume fraction (26%) of tested material [23]. The outer part of the model, where the grain shape is not simulated, has the averaged stiffness in the xy-plane. Finite element meshes consists of 4-nodes quadrilateral elements and few triangular elements. The size of element on a side is around 0.05mm near the grain-boundary, and around 0.01mm near the crack propagation path. The number of nodes is around 70,000. The [001] direction of each grains are set to be perpendicular to the surface in this analysis.

Analysis (iii) provides J of straight crack in homogeneous material. The crack direction is perpendicular to the load axis.

Analyses are conducted for various crack lengths from 0.675mm to 4.000mm with the increment of about 0.025mm. J is evaluated by the region integration method [24].

J-integrals obtained by analyses (i), (ii) and (iii) are denoted by J_{aniso}, J_{iso}, and $J_{straight}$, respectively.

In order to examine the effect of grain arrangement on the stress distribution of the material, an additional analysis with actual grains is conducted on the body without the crack and notch. Here, the notch is filled up by the material with the averaged stiffness.

ANALYTICAL RESULTS

Figure 3 shows σ_y under the remote tension of 400MPa in the uncracked body with the actual grains. σ_y fluctuates from 200 to 700MPa (Fig. 3(a)). Figures 3(b) and 3(c) show the magnified views near the highest stress point. The solid and dotted arrows in the figures show the crystallographic directions of <100> and <110>, respectively. The former has the lowest young's modulus, while the latter has the highest in the xy plane.
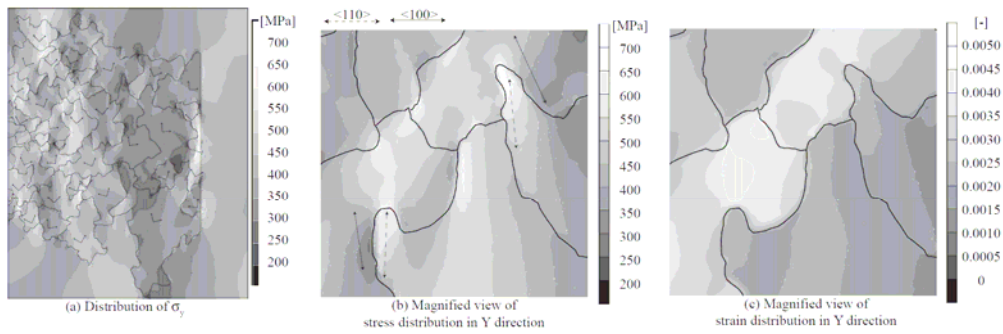
Fig. 3 Stress and strain distribution due to the anisotropic elasticity of grains

The maximum stress appears in a grain with the crystallographic direction of around <110> surrounded by the grains around <100>. According to the constraint of deformation, the center grain shows relatively high stress and low strain.

Figure 4 shows the change in the magnitudes of J_{aniso} and $J_{straight}$ against the crack length a. Although both show the similar trend in global, J_{aniso} exhibits the sporadic decrease to 1/2 to 1/3 of the average. The sketch of grain arrangement near the crack is shown in Fig. 4, where the cross point of grain-boundary and crack path is indicated by vertical solid line and the grain-boundary cracking is indicated by the hatching. The stepwise fluctuation, which can be seen in Fig. 4, corresponds to the grain arrangement. It is due to the differences in the elastic modulus of the grain in the macroscopic loading axis at the crack tip.
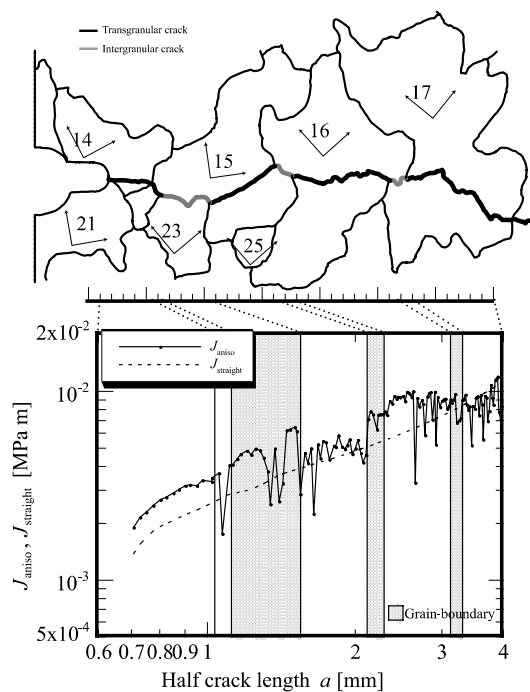

Fig. 4 Changes in magnitude of J_{aniso} and $J_{straight}$

Figure 5(a) shows the change in the magnitude of J_{iso} comparing with that of $J_{straight}$ against the crack length a. This shows the effect of microscopic inclination of crack shape on J. J_{iso} roughly corresponds to $J_{straight}$, while J_{iso} shows the sporadic decreases. The sporadic decreases in Figs. 4 and 5(a) are caused by the crack shape. The gray-colored solid line in Fig. 5(a) shows the profile of crack path. It can be seen that J_{iso} decreases when the crack path inclined largely apart from the macroscopic crack propagation direction. More precisely, this occurs when the microscopic crack direction deviates more than 40 degree from the macroscopic one. As such regions are less than 10% of total crack path, the crack shape gives limited effect on the magnitude of J.

The ratio, J_{iso} / $J_{straight}$, represents the effect of microscopic crack shape. Therefore, dividing J_{aniso} by the ratio,

$$J_{grain} = \frac{J_{aniso}}{J_{iso}\big/J_{straight}} \tag{1}$$

may give the effect of microstructural deformation on J. Figure 5(b) shows the relationship between J_{grain} and a. While it is continuous in a grain, it jumps when the crack crosses a grain-boundary. J eminently fluctuates at the grain-boundary cracking. It is attributed to the constraint of deformation due to neighboring grains. Since the stress fluctuates near a grain-boundary as shown in Fig. 3(b), J also fluctuates in the same manner. The largest peak in J indicated by solid arrow in Fig. 5(b) is observed near the grain-boundary with an acute shape, where the stress concentration is relatively high.
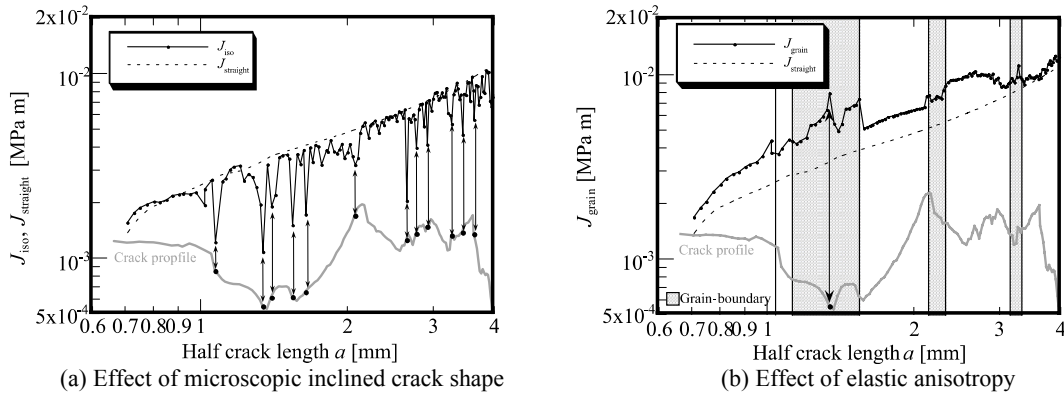

(a) Effect of microscopic inclined crack shape   (b) Effect of elastic anisotropy

Fig. 5 Effect of microscopic inclined crack shape on J

COMPARISON OF RESULTS WITH EXPERIMENTS

Figure 6 shows the relationship between the crack propagation rate da/dN (obtained by the fatigue crack propagation test) and J_{grain} (obtained by the analyses). The transgranular cracks fall in a single da/dN-J_{grain} relationship. The plots of intergranular cracks are categorized into 2 groups. One is on the same da/dN-J_{grain} relationship on that

in the transgranular cracks, and the other shows far higher *da/dN* than those in the transgranular cracks. The crack propagation rate of the latter group is around 3 to 5 times faster than that in the transgranular one. This group corresponds to the peak *da/dN* in Fig. 2 (*a*=1.3mm). Since the crack propagation rate is governed by the relative magnitude of crack driving force against the crack propagation resistance of the material, it is suggested that the increase of crack propagation rate here is caused by decrease of crack propagation resistance at the grain-boundary.
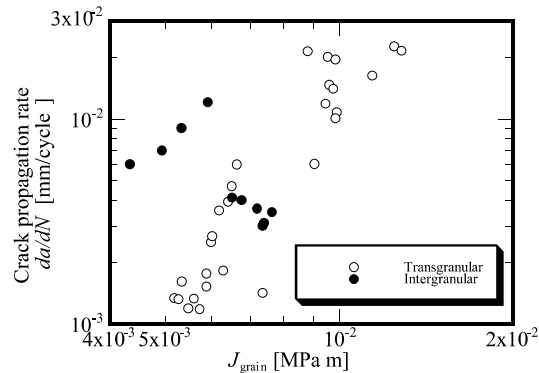

Fig. 6 Comparison of crack propagation rates in various microscopic crack paths

CONCLUSIONS

The effects of microscopic inhomogeneities on the crack driving force (J-integral) are investigated in fatigue of a directionally solidified (DS) superalloy using finite-element-analyses (FEA). The actual grain arrangement (grain shape and its anisotropic elastic stiffness) and the microscopic inclination of crack shape are modeled in the FE-models. Three types of *J*, such as J_{aniso}, J_{iso}, and J_{grain} are calculated, where J_{aniso} takes into account the both effects, J_{iso} does only the effect of latter, and J_{grain} does only the effect of former. The followings are summary of the analytical results.

1. The stress in the actual grain arrangement is fluctuated due to the difference of elastic modulus in the stress-applied-direction. The highest stress appears at the grain with high elastic modulus surrounded by the ones with the low elastic modulus.
2. J_{iso} shows the sporadic decrease when the microscopic crack inclines largely (> 40 degree) from the macroscopic propagation direction.
3. The elastic modulus of each grain brings about the stepwise change in J_{grain}.
4. The fluctuation of J_{grain} at intergranular crack indicates that the crack driving force depends on the relative stress / strain constraint near the grain boundaries. The highest peak of J_{grain} is at the point where the grain has acuminate shape.
5. *da/dN*-J_{grain} relationship of transgranular crack falls into a single line. This suggests that the fluctuation of crack propagation rate in the transgranular cracking is caused by the difference in the driving force. On the other hand, *da/dN* in the intergranular crack

shows the eminent acceleration. It suggests the lower crack propagation resistibility at the grain-boundary than that inside of the grain.

REFERENCES

1. Floreen, S., Kane, R. H. (1973) *Procs. of Fourth Int. Symp. on Superalloys, 595-604*
2. Shahinian, P., Sadananda, K. (1984) *Procs. of the Fifth Int. Symp. on Superalloys*, 741-750
3. Hoffelner, W. (1984) *Procs. of the Fifth Int. Symp. on Superalloys*, 771-783
4. Kamaya, M., Kitamura, T. (2005), *Int. J. of Fracture* **124**, 201-213
5. Ohtani, R., Kitamura, T., Tada, N. (1991), *Mat. Sci. and Engng.* **A143**, 213-222
6. Ohtani, R., Kitamura, T., Miki, H. (1991), *J. of Mat.Sci. Japan* **40-457**, 1297-1302
7. Ohtani, R., Kitamura, T. Tsutsumi, M., Miki, H. (1993), *Trans. of Japan Soc. of Mech. Engng.* **59-560**, 933-938
8. Anton, D. L. (1984), *Acta Mtell.* **32**, 1669-1679
9. Chan, K. S., Leverant, G. R. (1987), *Metall. Trans. A* **18A**, 593-602
10. Lerch, B. A., Antolovich, S. D. (1990), *Metall. Trans. A* **21A**, 2169-2177
11. Lupinc, V., Onfrio, S. (1995), *Mat. Sci. Engng.* **A202**,76-83
12. Henderson, M. B., Martin, J. W. (1996), *Acta Materialia* **44-1**, 111-126
13. Telesman, J., Ghosn, L.J. (1996), *ASME J. Engng. for Gas Turbines and Power* **118**,399-405
14. Pommier, S., Prioul, C., Bompard, P. (1997), *Fat. Fract. of Engng. Mat. Struct.* **20-1,** 93-107
15. Schubert, F., Rieck, T., Ennis, P. J., *Procs. ninth Int. Symp. on Superalloys,* 341-346
16. Müller, S., Rösler, J., Sommer, C., Hartnagel, W. (2000), *Procs. of the 9th Int. Sym. on Superalloys*, 346-356
17. Gopala Krishna, M. S., Sriramamurthy, A. M., Radhakrishnan, V. M. (1996), *Scripta Materialia* **35-11**, 1325-1330
18. Okada, M., Tsutsumi, M., Kitamura, T., Ohtani, R. (1996), *Fat. Fract. of Engng. Mat. Struct.* **21,** 741-750
19. Okada, M., Tsutsumi, M., Kitamura, T., Ohtani, R. (1996), *Fat. Fract. of Engng. Mat. Struct.* **21,** 751-760
20. Yamamoto, M., Kitamura, T. (2006), *Fat. Fract. of Engng. Mat. Struct.***,** accepted
21. Rice, J. R. (1968), In: *Fracture*, pp.191-311, Liebowitz, Academic Press, New York
22. Pollock, T. M., Argon, A. S. (1994), *Acta Metall. et Materialia* **42**, 1859-1874
23. Yaguchi, M., Busso, E. (2005), *Int. J. of Solid and Struct.* **42**, 1073-1089
24. Parks, D. M. (1974), *Int. J. of Fracture* **10-4**, 487-502